Development of an Algorithm of Dynamic Gridding for Multiphase Flow Calculation in Wells

C.C. Dong, M. Bahonar, Z. Chen, and **J. Azaiez,** University of Calgary

Summary
Because more and more wells have been put in operation, an accurate modelling of wellbore flow plays a significant role in reservoir simulation. One requirement of a wellbore model is its ability to trace various flow boundaries in the tubing, such as those created by phase or flow regime changing. An algorithm of dynamic gridding is applied to the wellbore flow model coupled with Stanford's general purpose research simulator (GPRS), which has the capability to simulate the isothermal black oil reservoir model to obtain detailed information that explains such important quantities as flow pattern and mixture velocity in any specific location of wellbore. A significant problem in this case is how to calculate fluid and velocity properties with a fine grid (segment) on the boundaries of different flow regimes in the wellbore. Local dynamical segment refinement in the well can accurately and effectively handle this problem. This wellbore model includes mass conservation equations for each component and a general pressure drop relationship. The multiphase wellbore flow is represented using a drift-flux model, which includes slip between three fluid phases. The model determines the pressure, mixture flow velocity, and phase holdups as functions of time and the axial position along the well or alleviation depth. In addition, this model is capable of generating automatically adaptive segment meshes. We apply the black oil model to the simulation of several cases of isothermal dynamical local mesh refinement, and compare the results with fixed coarse and fine meshes. The experiments show that using local segment refinement can yield accurate results with acceptable computational time.

Introduction
After the boom in oil and gas production in the late 20th century, the number of wells drilled has increased substantially; currently, thousands of wells are being drilled in the globe annually. Meanwhile, new sophisticated wells, such as deep vertical or inclined wells, long horizontal wells, complex multilateral wells, and multitubing wells, have emerged. The purpose of developing these wells is to access more difficult hydrocarbon-formation locations in addition to acquiring greater control on wellbores and reservoir formations.

In the course of well development, modelling and simulation techniques have also grown quickly. This growth has mainly been accelerated by Ramey (1962), who proposed the first mathematical model to estimate the fluid temperature as a function of the well depth and production time for hot water injection. Although Ramey used several assumptions in his model, his pioneer work was the basis of many other subsequent developments; many different investigators attempted to relax Ramey's assumptions and even made their models more sophisticated to be able to model the new emerging complex wells. Wellbore flow modelling has been found to have diverse applications not only in the petroleum industry, but also in other industries. Some of these applications can be found in our recent papers (Bahonar et al. 2010a, 2010b).

Generally, wellbore models involve the mass, momentum and energy (if the system is nonisothermal) conservation equations inside the tubing along with the use of an equation of state and other multiphase flow equations. These multiphase flow equations have significant effects on the prediction capability of any wellbore simulator and largely affect the estimation of fluid properties such as phase densities, gas in-situ volume fraction, velocities, and pressure drops. Because of these reasons different classes of multiphase flow equations have been proposed during the last few decades. These equations can be mainly divided into two large groups: empirical correlations and relatively new and advanced mechanistic models.

The first group comprises three different categories. The first category includes those unrealistic correlations that consider the whole flow to be homogenous. These correlations assume no-slip flow and there is no flow pattern consideration in this category. Examples are those by Poettmann and Carpenter (1952) and Baxendell and Thomas (1961). The latter includes those that consider the slip phenomenon, but there is no flow pattern consideration such as the one by Hagedorn and Brown (1965).The last category in this group includes those correlations that consider both the slip phenomenon and flow pattern. Famous examples in this category are those by Duns and Ros (1963) and Beggs and Brill (1973). One of the drawbacks of all these correlations is that their prediction is confined to the range of the experimental data on which these correlations were based.

The second group involves the flow pattern-based mechanistic models that are based more on the physics of the underlying problem and thus are applicable to a wider range of situations in contrast to the correlations in the first group. Examples are the methods of Ansari et al. (1994) and Hasan et al. (2007). Of the powerful models in the second group is the drift-flux model (Hasan et al. 2007 and Shi et al. 2005a). This drift-flux model has been successfully employed by industry in various applications (e.g., ECLIPSE Reservoir Simulation Software) because of its simplicity and accuracy. In this model, it is considered that the gas phase moves faster than the liquid phase because of buoyancy (i.e., tendency of gas to rise vertically through a liquid) and its tendency to flow close to the pipe centre, in which the local mixture velocity is the fastest. Hence the in-situ gas velocity is the sum of the bubble rise velocity, v_∞ and the pipe centre mixture velocity, $C_o v_m$ (i.e., the maximum velocity). Using the definition of the gas velocity, $v_g = q_g/A_g = (q_g/A)/(A_g/A) = v_{sg}/f_g$, the generalized form of the in-situ gas volume fraction for a production well is:

$$f_g = \frac{v_{sg}}{C_o v_m + v_\infty}, \quad (1)$$

where the values of the profile parameter, C_o and the rise velocity, v_∞ depend on the flow direction and flow pattern. The profile parameter is usually assumed to be 1.2 for the bubble and slug flow regimes, but 1.0 or close to 1.0 for the annular flow regime. C_o also approaches 1.0 as the flow becomes the single-phase gas. The pro-

 This paper was accepted for presentation at the CPS/SPE International Oil and Gas Conference and Exhibition in China held in Beijing, China, 8–10 June 2010, and revised for publication. Original manuscript received for review 16 June 2010. Revised paper received for review 18 September 2010. Paper peer approved 15 September 2010 as SPE Paper 131019.

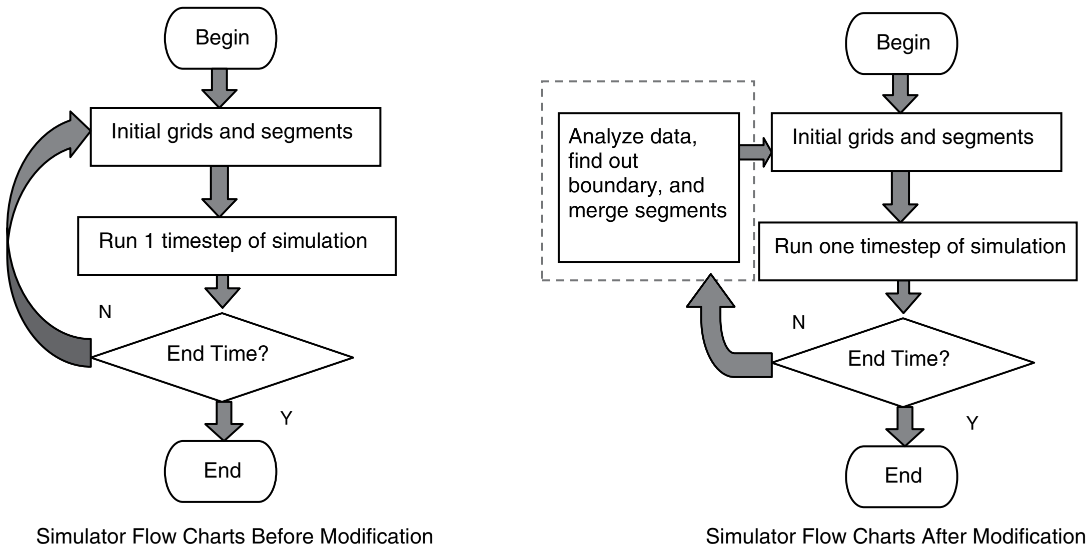

Fig. 1—The flow charts of modifying GPRS with dynamic segment implementation.

file parameter C_o and the rise velocity v_∞ are estimated based on some correlations that have been tuned by experimental data for each flow regime. However, the values of these parameters at transition regimes are estimated based on the interpolation between the values of adjacent flow regimes to preserve the continuity and differentiability of the drift-flux model. The interpolation technique can be linear (Shi et al. 2005a and 2005b), exponential (Hasan et al. 2007) or any other appropriate and arbitrary scheme.

Using the dynamical local grid refinement method to be able to trace the boundary motion in reservoir simulation has been an issue. The main benefit of using this method is to overcome unexpected results caused by the use of large grid size (Ding and Lemonnier 1993), together with the necessary time spent only for dynamic local refinement on the required fine meshes (Han et al. 1987).

For a flow regime change, some value for the in-situ gas volume fraction f_g is assumed as the transition criterion. However, if large grid (segment) blocks are considered in the wellbore to speed up computations, the transition process from one flow regime to another may not be described accurately. Overall grid refinement increases the computational time of the simulator. Therefore, we implement the idea of dynamical gridding into a recently developed coupled wellbore/reservoir simulator called General Purpose Research Simulator (GPRS). This simulator is based on the drift-flux model proposed by Shi et al. (2005a and 2005b). The idea is to run the simulator with coarse segments at the first iteration and track the segments where the transition occurs and that are refined at the next timestep. This scheme allows us to use coarse segments for the wellbore to complete fast computations and meanwhile, maintain the accuracy of the multiphase flow equations by tracking the transition zones with local dynamical segments refinement.

In the next sections, we will describe the algorithm and implementation of dynamical local segments refinement into GPRS and the results.

Implementation of Wellbore Model

The wellbore model's basic equations are based on mass conservation and pressure drop equations. The pressure drop on one segment

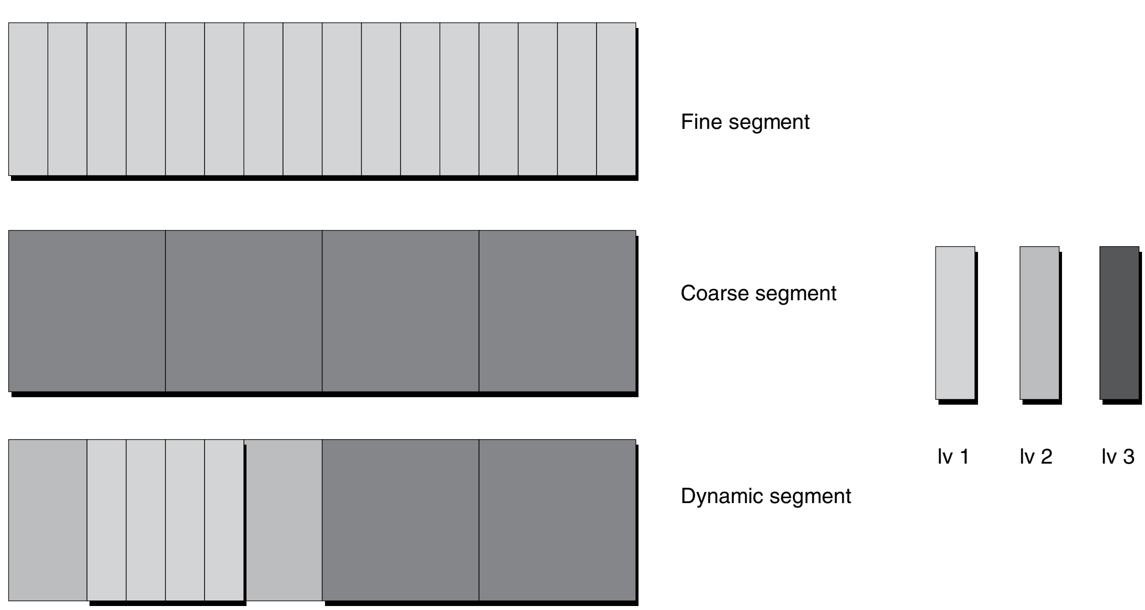

Fig. 2—Fine, coarse, and dynamic segments.

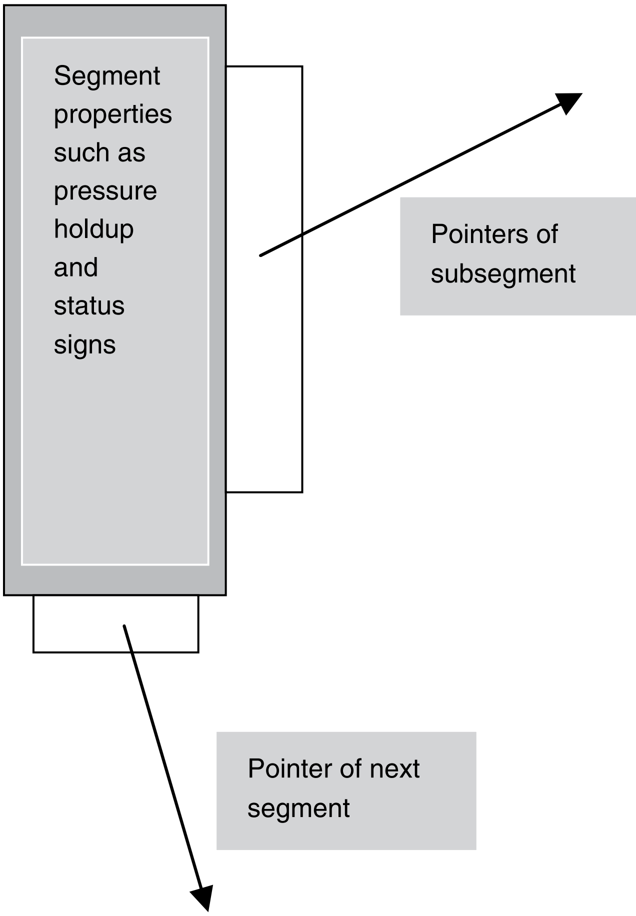

Fig. 3—The structure of nodes.

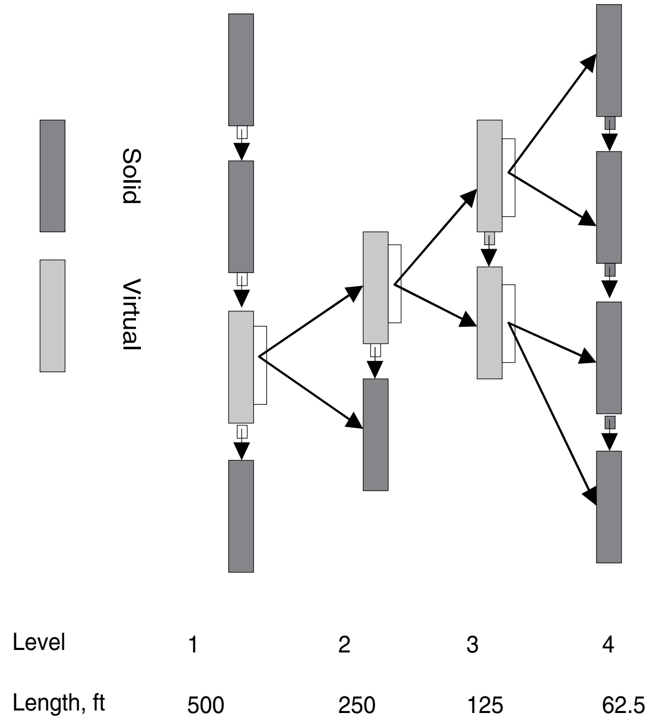

Fig. 4—Using nodes to present a 1D dynamical multisegment wellbore.

is divided into three parts: hydrostatic, frictional, and acceleration or kinetic pressure lost. All these equations can be found in Livescu et al.'s (2010) paper. After we attach an adaptive segment mesh procedure and its corresponding data structure at every timestep end of GPRS, a wellbore discretized algorithm with dynamical local segment refinement ability is constructed **(Fig. 1).** We will demonstrate how we construct the adaptive mesh segments both functionally and data-structurally next.

Data Structure. To create a multisegment well model, the wellbore domain is preliminarily meshed with a series of cylindrical segments. These fixed segments are coarse segments or base segments. We will automatically refine them along the wellbore to construct dynamical local refined segments as simulation progresses. To compare the efficiency and accuracy of different segment construction approaches, a finest segment mesh with uniformly refined segments that have the same properties as those for the smallest segment in the domain of dynamical local refined segments has also been created.

In the dynamical refining scenario, each segment can be divided into a predetermined number of subsegments; all those subsegments can also be divided into pieces determined by both adjoined segment properties and the level of refinements. An example of coarse, fine, and dynamic segments is shown in **Fig. 2.**

Data structure and segment management used in this system are designed to ease their implementation in GPRS. All algorithms are implemented in the C++ language. The ability of dynamical allocation, deleting memory, and recurrence makes C++ efficient and easy to construct the dynamical meshing scenario. The data structure is based on nodes. The nodes contain properties such as pressure, holdups, and densities. Information associated with segments structure, constructed by pointers being pointed to other nodes, is also included in the nodes. Some status factors, such as the level of refinements, virtual, or solid segments, are also stored in the nodes. The structures of nodes are illustrated in **Fig. 3.**

In order to simplify the presentation of the data structure, a four-level case will be considered. The demonstration of the data structure is shown in **Fig. 4.** In this case, a 2,000-ft-long wellbore has local segment refinement to four 500-ft-long base segments. After that, a local refinement divides the third segment into two subsegments, then the first subsegments are refined into two pieces, and finally these two pieces are subdivided into segments containing a length of 62.5 ft at the level of four. In this case, the wellbore are finally divided into three 500-ft segments, four 62.5-ft segments, and one 250-ft segment; other nodes are virtual and are not considered in the calculation process, and are only reserved for a future process such as dynamic local refinement or for the merging process. In summary, we have a three-level well partition with a maximum of eight segments using a dynamic scheme compared to the four-segment coarse grid configuration and 16-segment fine-grid well construction.

Algorithm of Dynamic Local Segments Refinement. Recurrence is used in order to implement the algorithm; a pseudocode is provided here for further information. The algorithm begins with checking the flow regime status for each solid segment, then goes through the nodes of the original segments' list to determine if the segments need local refinement, and then goes through the nodes again to merge the necessary subsegments. Numerical values of properties are updated easily in each refining process based on the value of the father segments with respect to gravity; for the merging-segment process, this algorithm updates the assembled segments' fluid properties with the averaged values of fluid properties, such as holdups and densities, and sums the wellbore geological properties, such as length, as assembled segments; the pressure of assembled segments can be assigned as the toe segments for the purpose of GPRS configuration.

Careful memory storage minimization is obtained by adding the nodes from the refinement process and deleting the nodes related to

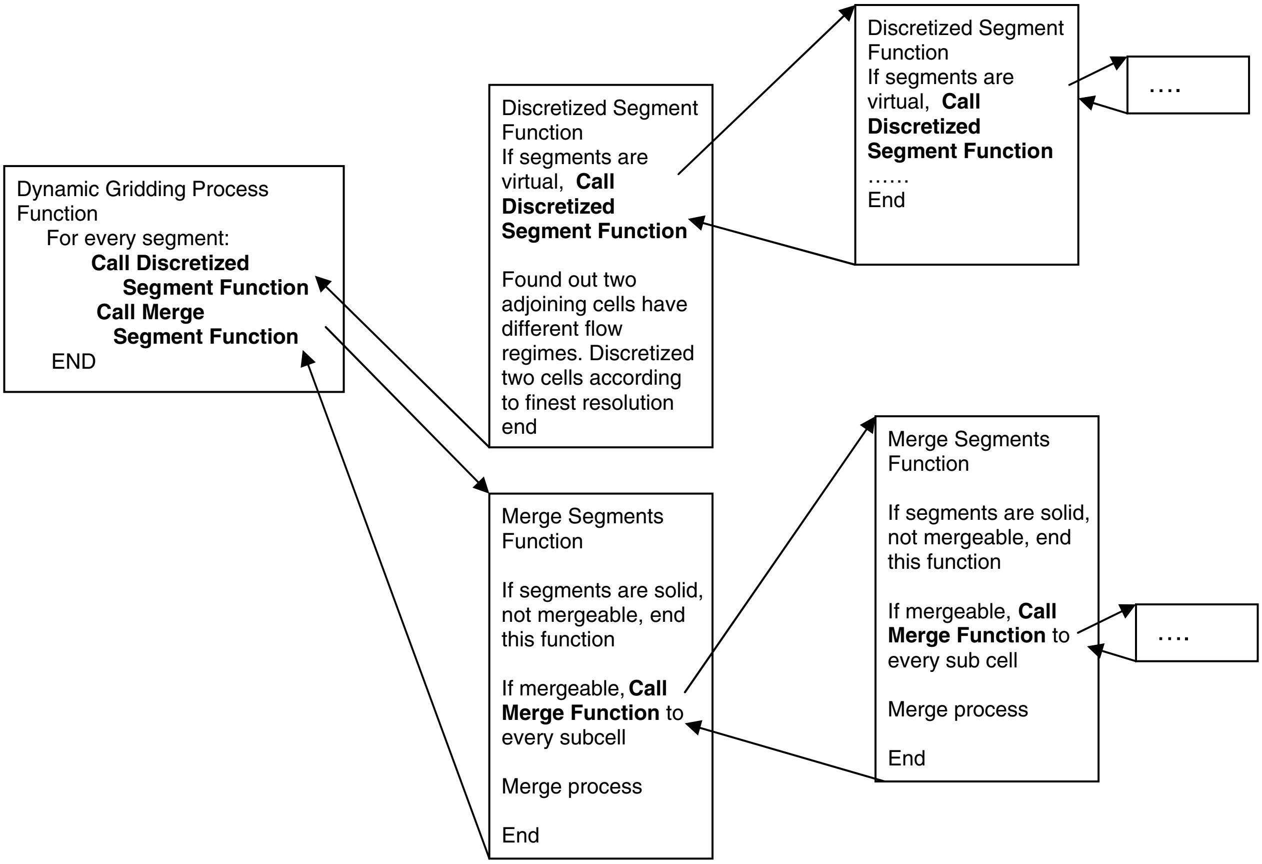

Fig. 5—Demonstration of a dynamic gridding algorithm.

the merged subsegments. In the refinement process, both segments near the flow regime's changing boundary are found using the recurrence and reference method in C++, refined, and allocated with new nodes to store the subsegments' information. In the merging process, the nodes that no longer exist are deleted first, and then the property storage in these nodes is automatically set free by this process. The cell neighbours can be easily found using the recurrence and reference method provided by C++.

The dynamical local segment refinement must be applied at flow regime boundaries to improve accuracy of the solution. The position of the flow regime boundaries can be located by going through nodes recurrently. Once the boundaries have been located, the neighbouring solid segments are refined into a set of subsegments.

The initialization of dynamic grids needs a small timestep trial run on the base or coarse grid to find the flow regime the first time. When we locate the regime-changing boundary, the dynamic local grid refinement process will divide its segments to subsegments, with the grid size increasing at the regions away from this changing boundary. The balanced refined grid contains different sizes of grids, and this procedure is terminated by a preset maximum number of recurrences. As shown in Fig. 2, if the boundary is found to be located between the first and second segments of the basecase, the discretized segments are only shown as the fine grid.

A dynamic gridding process is given in **Fig. 5.** The algorithm calls the discretization process recurrently to find the adjoining flow regime-changing segments, and then discretizes them by using the method previously mentioned. After the discretization process, a merging process is also called to merge the same flow regime subsegments recurrently until the boundary or base segment contains exclusively only the discretized segments.

Results and Discussions

Case 1. Adaptive segments' refinement accurately and efficiently describes the phase change. In a wellbore, two-phase flow and three-phase flow regimes can coexist when pressure goes through the bubblepoint. The first case involves a 2,000-ft vertical production well originally discretized into two segments as coarse segments; we also built a series of uniformly refined segments from 2 to 512 segments as comparable fine segments. Dynamical local segment updating can be as high as eight levels with two subsegments each uniformly refined. The wellbore model is fully coupled with a 3D coarse reservoir model that has $3\times3\times1$ grids and a gridblock size 1,000 ft for depth, width, and length. Although there is a reservoir-wellbore calculation issue as a result of coarse grid selection for the reservoir, this effect is ignored because our main concern is with wellbore regime. If a finer reservoir grid is used, it will increase the overall accuracy of the coupled wellbore/reservoir simulator; however, in this case we may not be able to clearly distinguish between the computational times that are used by each wellbore gridding scheme. Therefore, a coarse reservoir grid was implemented only for comparison purposes. Fluid and rock property data are from SPE10; three fluid phases coexist both in the reservoir and wellbore. The linear system is solved with the generalized minimal residual (GMRES) method with a constraint pressure residual (CPR) preconditioner for advanced wells. The gas holdup value is chosen as the boundary tracking criterion. In this case we keep the constant timestep at 0.1 days in all coarse, fine, and dynamical segment runs (the simulation end time is set to 160.1 days) in a dual-2.99 GHz CPU, 3.24 GB ram system to compare the efficiency difference. The results are shown in **Fig. 6** and **Table 1.** From the results we can see that the Newton and solver iterations did not change much with respect to the segment's number. Thus we can say that the reason of significant efficiency differences is mainly caused by the time differences consumed at solving the Jacobian matrices with different dimensions. For the eight-level dynamical segmenting refinement, the averaged segment's number over the whole domain is approximately 11 segments. The memory storage shows no evidence of significant growth.

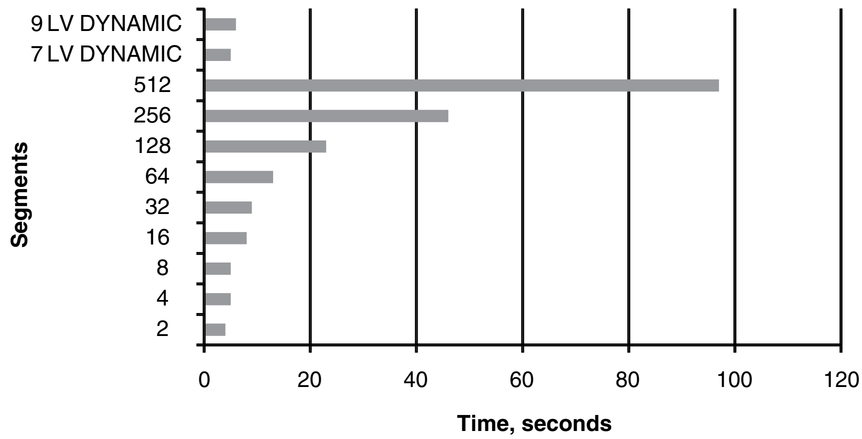

Fig. 6—Time spent differences with two to 512 fixed segments and seven- to nine-level dynamical segments.

TABLE 1—TIME COMPARISION FOR TWO-, FOUR-, EIGHT-, 16-, 32-, 64-, 28-, 256-, 512-, SIX-LEVEL DYNAMIC, AND EIGHT-LEVEL DYNAMIC SEGMENTS AS RUN TO 160.1 DAYS WITH CONSTANT TIMESTEP OF 0.1 DAYS

Segment Type	Time, seconds	Newton Iteration Number	Solver Iteration Number
2	4	5,774	19,304
4	5	7,762	24,884
8	5	8,988	28,563
16	8	9,348	29,642
32	9	8,415	26,844
64	13	8,017	25,650
128	23	8,016	25,647
256	46	8,016	25,647
512	97	7,985	25,554
6 LV DY	5	8,945	27,843
8 LV DY	6	9,045	28,476

The second part of this case has the same physical data as the first part, but we changed the time scale to the logarithmic one to compare the accuracy of coarse, fine, and dynamical segments. In this part, the timesteps are arranged from 0.0001 to 10 days for the first six timesteps, and then are increased from 10 to 70 days. In this period of time, both the bubble flow and two-phase (oil and water) liquid flow exist in the wellbore. For the wellbore division, we chose four uniformly refined segments as the base segments and 512 uniformly refined segments as the finest segment setting; a seven-level dynamical local segment refinement was used. The segments generated by this scenario have a segment size between the coarsest and finest segments. The results of the mixture velocity profiles predicted by different segment constructions are shown in **Figs. 7 and 8.** As is shown, there is a large deviation between the coarse and fine segments. Using the dynamical approach we can eliminate this difference. The phase's holdup differences at 0.01 days are plotted in **Fig. 9.** The reason for high-oil density and low-gas fraction changes is the pressure difference of 5 psi, in total 4,767 psi, at the wellhead between the coarse and fine segments. We also studied this case by tracing the flow regime-changing phenomenon—a plot of the bubblepoint position traced by different segment constructions with calculations by averaging the adjoining flow regime changing points with respect to time, as shown in **Fig. 10.** Finally, a wellbore mixture velocity profile predicted by dynamic local segment refinement is shown in **Fig. 11.**

Case 2. Deviated wells are also considered; here we take the same data set from Case 1 except for the wellbore construction at 45° inclined to the ground. Because of a longer wellbore length than in Case 1, the bubble drift can travel longer than in the Case 2 well configurations. Time spent is almost the same as in Case 1 with respect to different segment settings. But for the reason of a longer wellbore length and larger drift velocity, the profiles have significant differences between the coarse and fine divisions, as shown in **Figs. 12 and 13.** Dynamical local segment refinement plays a more sophisticated role shown in the results of this case.

Case 3. When the flow regime changes, the estimation of wellbore fluid properties is always challenging. The fourth case contains the same physical data as Case 3. It is intended to compare the dynami-

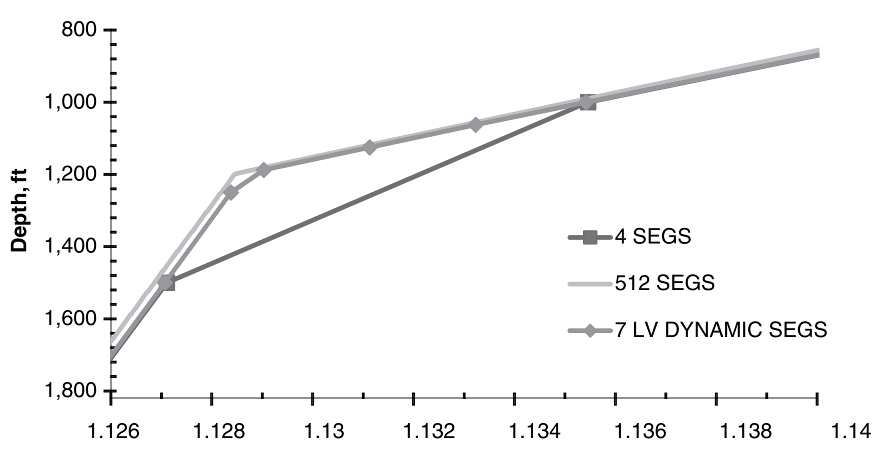

Fig. 7—Comparison between four-, 512-, and eight-level dynamic segments mixture velocity profiles at 0.1 days for Case 1.

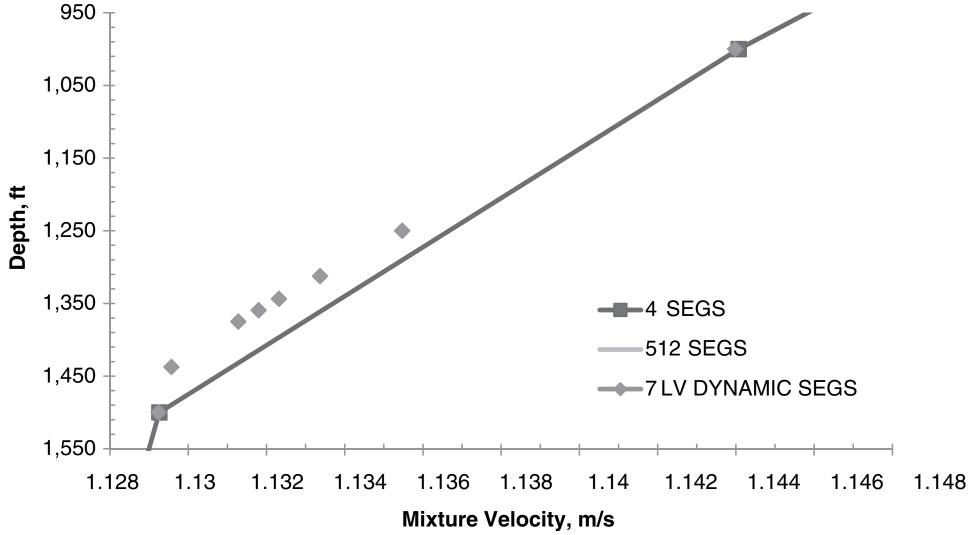

Fig. 8—Comparison between four-, 512-, and seven-level dynamic segments mixture velocity profiles at 50 days from 950 ft to 1,550 ft in depth for Case 1.

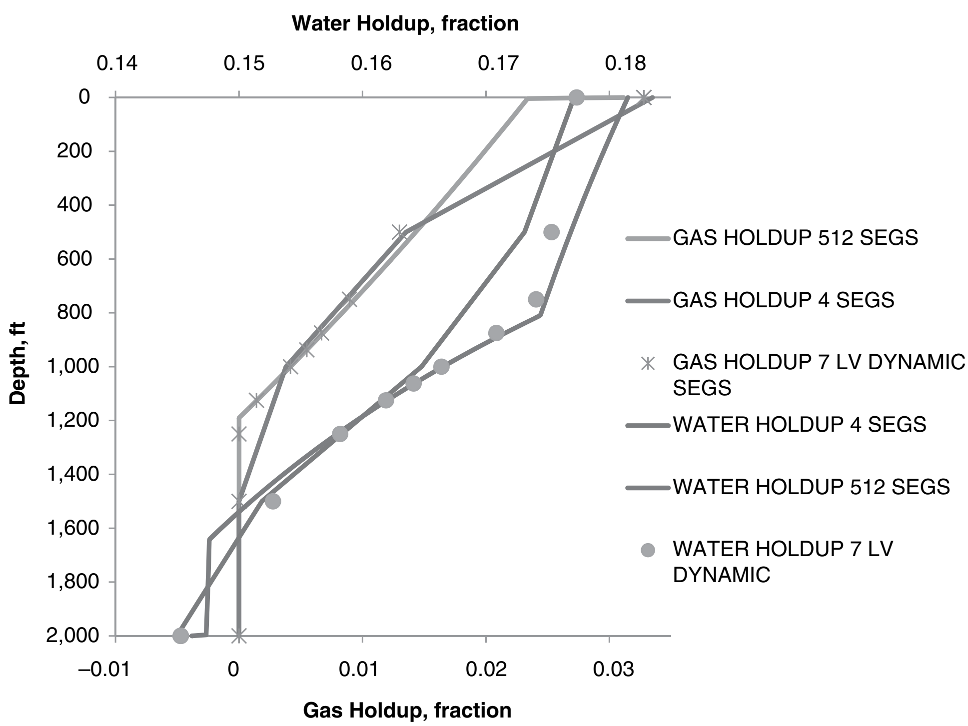

Fig. 9—Comparison between four-, 512-, and seven-level dynamic gas and water holdups at 0.01 days for Case 1.

cal local segments' refinement efficiency and accuracy when there is a flow regime change with both coarse and fine segments. The timestep of this case is chosen to be 10 days, and the simulation time is set as 2,000 days. The time efficiency for the four multisegment models and one seven-level dynamical segment model is almost the same, approximately 1 second. For the 512 segments' well configuration, it is 13 seconds. When the gas holdup in the wellbore ranges from 0 to 0.06 (fraction), the flow regime can be recognized as the bubble flow. When it is from 0.06 to 0.10 as a fraction, the regime is the transit flow. From 0.10 to 1 as a fraction, it is recognized as the slug flow. Some of the results are illustrated in **Figs. 14 and 15.** To compare the accuracy of dynamical local segment refinement with that of the coarse and fine segments, in Fig. 14 a flow regime changing from bubble to transit is captured and computed with less time, but greater accuracy, and in Fig. 15 a flow regime changing from transit to slug flows is also captured.

Conclusions

An algorithm of dynamic gridding applied to the wellbore flow model has been coupled with Stanford's GPRS. This model has been tested by using several test cases capable of dealing with vertical and deviated well situations to reduce computational time with acceptable accuracy when there are changing phases or flow regimes. We have obtained reasonable results with reduced simulation time. **JCPT**

Nomenclature

A = total area
A_g = area occupied by gas
C_o = distribution coefficient in the drift-flux model
DY = dynamic
f_g = gas in-situ volume fraction
Lv = level
q_g = gas flow rate

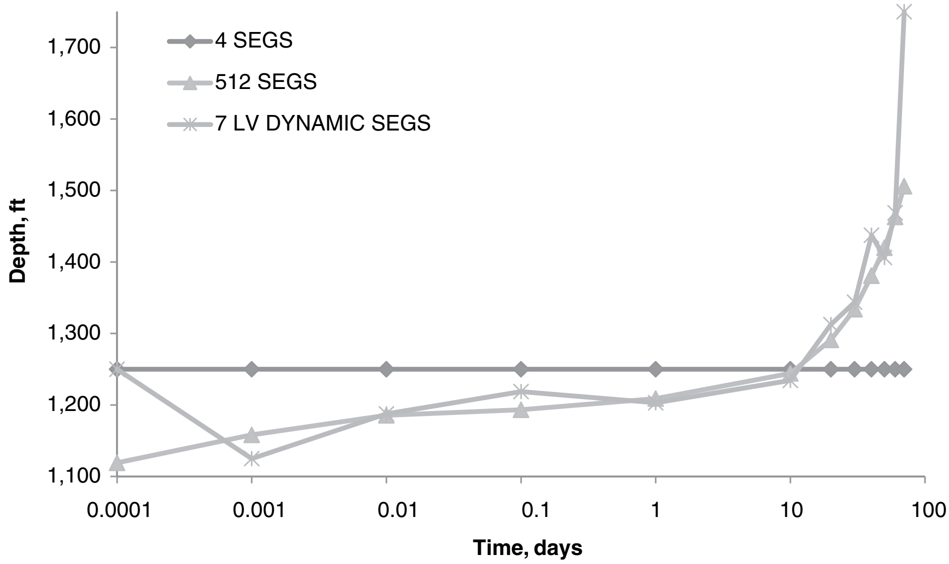

Fig. 10—Different segment construction flow regime changing estimation for Case 1.

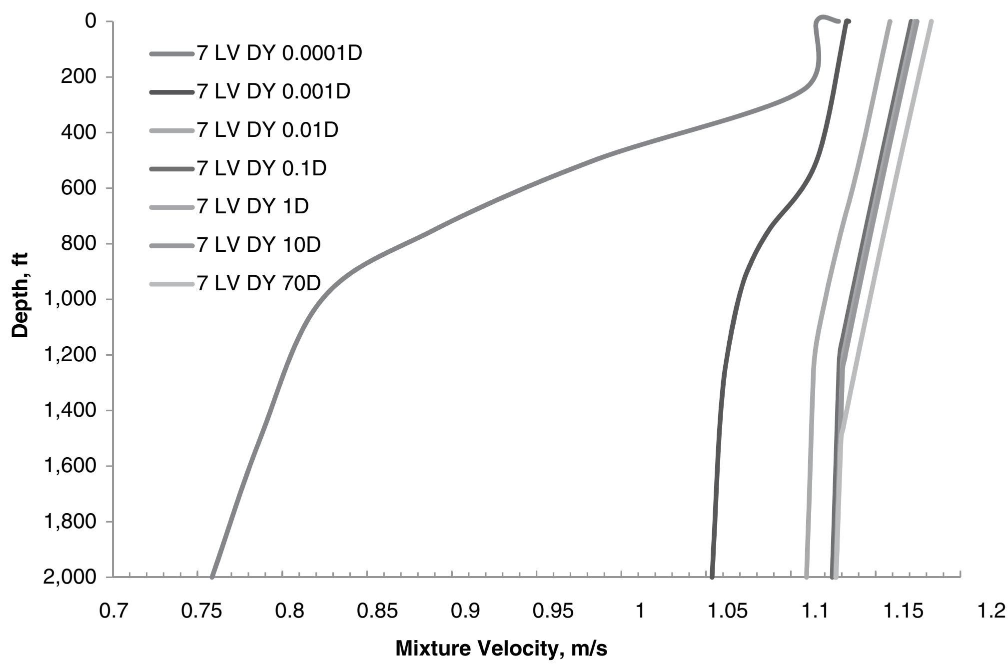

Fig. 11—Wellbore mixture velocity profiles predicted by seven-level dynamic segments for Case 1.

Seg = segment
v_g = gas velocity
v_L = liquid velocity
v_m = mixture velocity
v_{sg} = superficial gas velocity
v_{sL} = superficial liquid velocity
v_∞ = drift velocity of gas in liquid

References

Ansari, A.M., Sylvester, N.D., Sarica, C., Shoham, O., and Brill, J.P. 1994. A Comprehensive Mechanistic Model for Upward Two-Phase Flow in Wellbores. *SPE Prod & Fac* **9** (2): 143–152; *Trans.*, AIME, **297**. SPE-20630-PA. doi: 10.2118/20630-PA.

Bahonar, M., Azaiez, J., and Chen, Z. 2010a. *In press*. Overview of Wellbore Fluid and Heat Flow Modeling and its Applications in Oil Industry. *Exploration & Production: Oil & Gas Review* (accepted for publication in vol. 8, no. 2, 2010).

Bahonar, M., Azaiez, J., and Chen, Z. 2010b. A Semi-Unsteady-State Wellbore Steam/Water Flow Model for the Prediction of Sandface Conditions in Steam Injection Wells. *J Can Pet Technol* **49** (9): 13–21. SPE-140663-PA. doi: 10.2118/140663-PA.

Baxendell, P.B. and Thomas, R. 1961. The Calculation of Pressure Gradient in High Rate Flowing Wells. *J Pet Technol* **13** (10): 1023–1028; *Trans.*, AIME, **222**. SPE-2-PA. doi: 10.2118/2-PA.

Beggs, H.D. and Brill, J.P. 1973. A Study of Two-Phase Flow in Inclined Pipes. *J Pet Technol* **25** (5): 607–617; *Trans.*, AIME, **255**. SPE-4007-PA. doi: 10.2118/4007-PA.

Ding, Y. and Lemonnier, P.A. 1993. Development of Dynamic Local Grid Refinement in Reservoir Simulation. Paper SPE 25279 presented at the SPE Symposium on Reservoir Simulation, New Orleans, 28 February–3 March. doi: 10.2118/25279-MS.

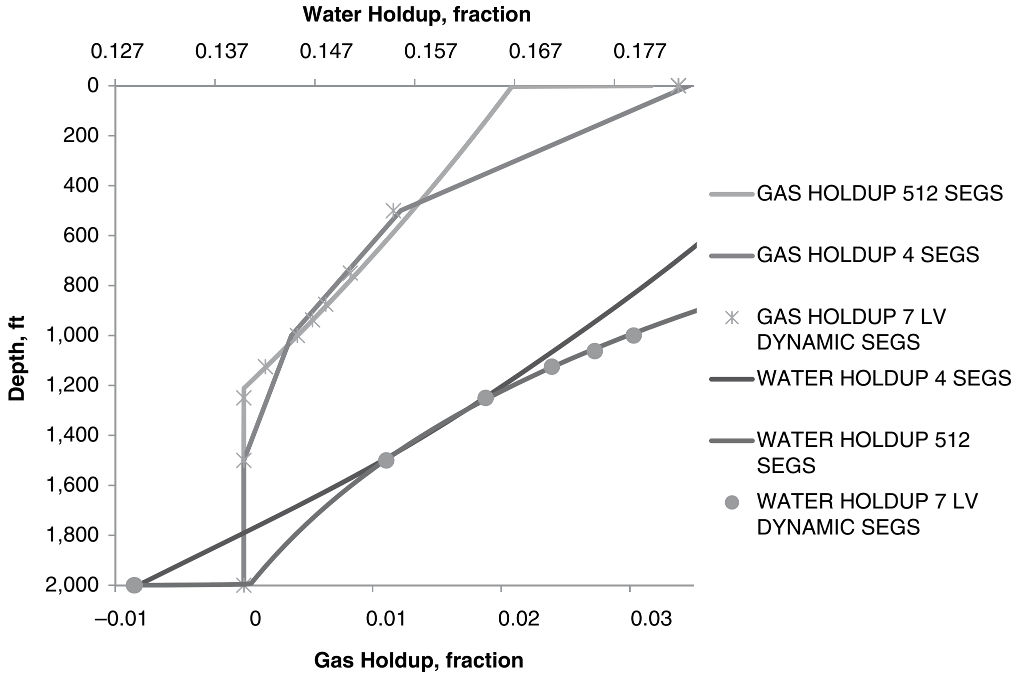

Fig. 12—Comparison between four-, 512-, and seven-level dynamic gas and water holdups at 0.01 days for Case 2.

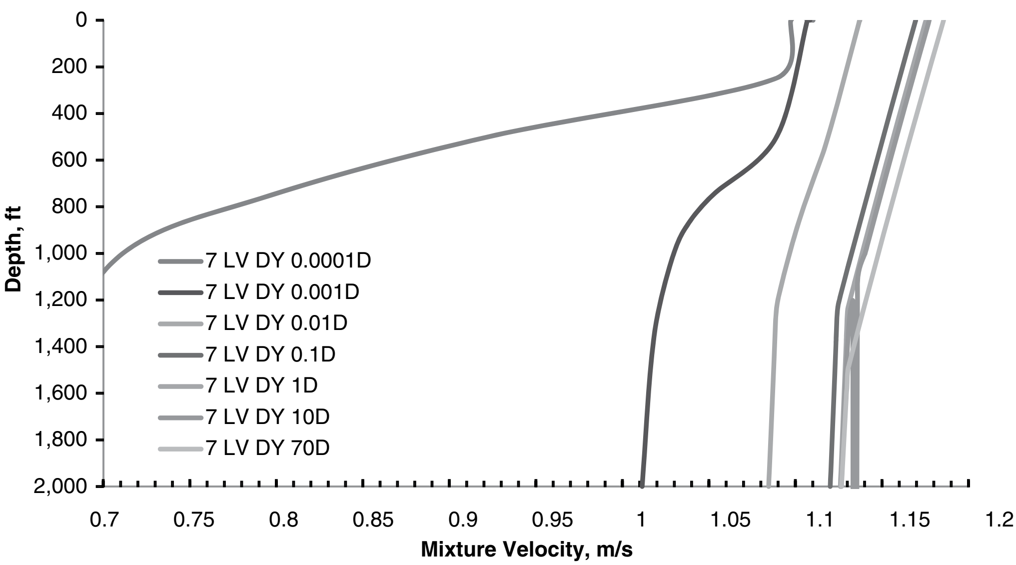

Fig. 13—Wellbore mixture velocity profiles predicted by seven-level dynamic segments for Case 1.

Duns, H. and Ros., N.C.J. 1963. Vertical flow of gas and liquid mixtures in wells. *Proc.*,6th World Petroleum Congress, Frankfurt am Main, Germany, Section II, 451-465.

Hagedorn, A.R. and Brown, K.E. 1965. Experimental Study of Pressure Gradients Occurring During Continuous Two-Phase Flow in Small-Diameter Vertical Conduits. *J Pet Technol* **17** (4): 475–484; *Trans.*, AIME, **234**. SPE-940-PA. doi: 10.2118/940-PA.

Han, D.K., Han, D.L., Yan, C.Z., and Peng, L.T. 1987. A More Flexible Approach of Dynamic Local Grid Refinement for Reservoir Modeling. Paper SPE 16014 presented at SPE Symposium on Reservoir Simulation, San Antonio, Texas, USA, 1–4 February. doi: 10.2118/16014-MS.

Hasan, A.R., Kabir, C.S., Sayarpour, M. 2007. A Basic Approach to Wellbore Two-Phase Flow Modeling. Paper SPE 109868 presented at the SPE Annual Technical Conference and Exhibition, Anaheim, California, USA, 11–14 November. doi: 10.2118/109868-MS.

Livescu, S., Durlofsky, L.J., Aziz, K., and Ginestra. J.C. 2010. A Fully-Coupled Thermal Multiphase Wellbore Flow Model for Use in Reservoir Simulation. *Journal of Petroleum Science and Engineering* **71** (3–4): 138–146. doi: 10.1016/j.petrol.2009.11.022.

Poettmann, F.H. and Carpenter, P.G. 1952. The Multiphase Flow of Gas, Oil and Water Through Vertical Flow Strings. *API Drilling and Production Practice* (1952): 257.

Ramey, H.J. 1962. Wellbore Heat Transmission. *J Pet Technol* **14** (4): 427–435; *Trans.*, AIME, **225**. SPE-96-PA. doi: 10.2118/96-PA.

Shi, H., Holmes, J.A., Durlofsky, L.J., Aziz, K., Diaz, L.R., Alkaya, B., and Oddie, G. 2005a. Drift-Flux Modeling of Two-Phase Flow in Wellbores. *SPE J.* **10** (1): 24–33. SPE-84228-PA. doi: 10.2118/84228-PA.

Shi, H., Holmes, J.A., Diaz, L.R., Durlofsky, L.J., and Aziz, K. 2005b. Drif-Flux Parameters for Three-Phase Steady-State Flow in Wellbores. *SPE J.* **10** (2): 130–137. SPE-89836-PA. doi: 10.2118/89836-PA.

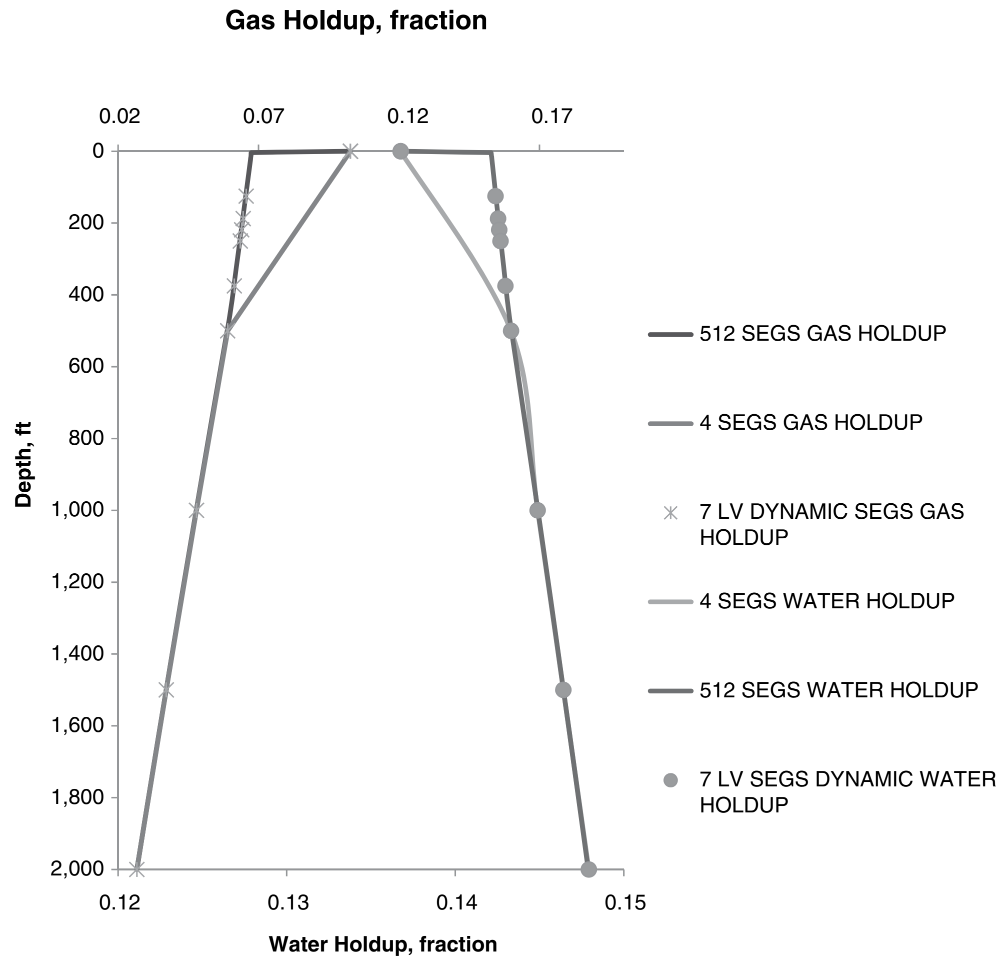

Fig. 14—Gas and water holdups profiles in wellbore at 300 days when bubble and transit flow coexist in the wellbore.

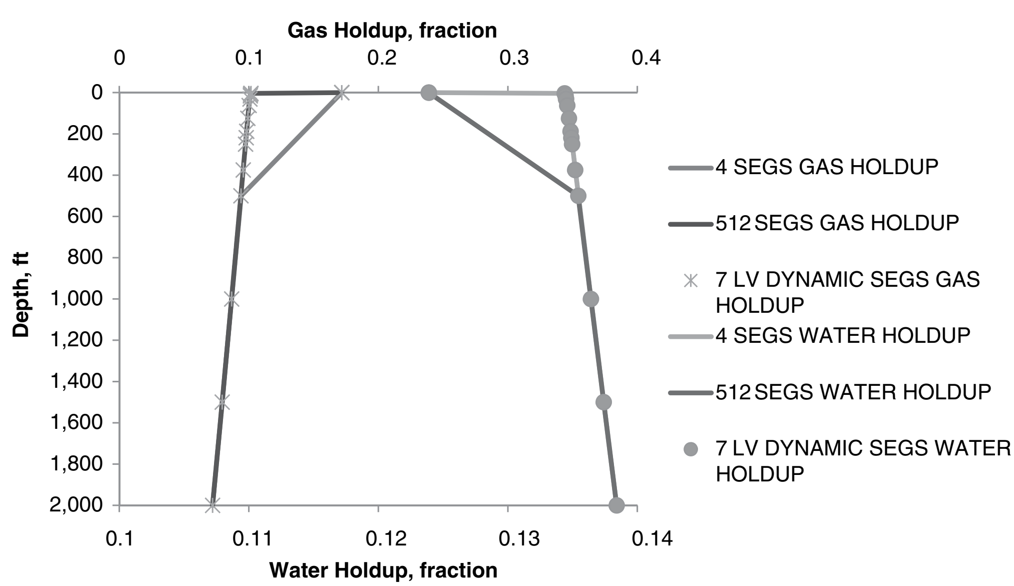

Fig. 15—Gas and water holdup profiles in wellbore at 480 days when transit and slug flows coexist in the wellbore.

Authors

Chao (Charlie) Dong is a Ph.D. candidate who joined the Department of Chemical and Petroleum Engineering at the University of Calgary in September 2008. Dong has conducted research that explains topics related to steam injection in a heavy-oil carbonate reservoir, looking at the modelling using computer science and mathematics models of fluid flow and heat transfer in coupled wellbore/reservoir systems. He holds a B.Eng. degree and a M.Sc. degree in the specification of optimization using genetic algorithms, both from Wuhan University in China.

Mehdi Bahonar is a petroleum engineering Ph.D. candidate who joined the department of chemical and petroleum engineering at the University of Calgary in September 2007. Bahonar has conducted research that explains topics related to steam injection in a fractured heavy oil carbonate reservoir in Iran, natural convection and thermal radiation in wellbore annulus, and is currently looking at the modelling of nonisothermal transient fluid flow and heat transfer in coupled wellbore/reservoir systems. Bahonar has received several academic awards, scholarships and bursaries (including the Alberta Ingenuity Ph.D. Graduate Student Scholarship) and authored or coauthored a number of technical and journal papers. He holds a B.Sc. degree in petroleum production engineering from the Petroleum University of Technology (PUT) in Iran and dual-M.Sc./M.Eng. degrees in reservoir engineering from the University of Calgary/PUT, both as the first top student. He is a member of SPE.

Zhangxin (John) Chen is currently a professor at the University of Calgary and director of Schlumberger iCentre for Simulation and Visualization. He also holds the NSERC/AERI/Foundation CMG Senior Research Chair in Reservoir Simulation, and the iCORE Industrial Chair in Reservoir Modelling. He formerly held a Tengfei Chaired and Chang Jiang Chaired Professorship at Xi'an Jiaotong University, the Tepin Professorship of Energy and Resources at the Peking University, the Ziqiang Professorship at Shanghai University, and the Gerald J. Ford Research Professorship at Southern Methodist University. He holds a B.S. degree from the University of Jiangxi, an M.S. degree from Xi'an Jiaotong University in China, and a Ph.D. degree from Purdue University. He is a member of SPE.

Jalel Azaiez is currently an associate professor at the Department of Chemical and Petroleum Engineering at the University of Calgary. He has published more than 40 refereed journal papers, published more than 20 refereed conference proceedings papers, and has given 55 conference talks. He has also presented nine invited talks and seminars worldwide. Azaiez's expertise is in the field of mathematical modelling and numerical simulation of fluid flows with a particular focus on complex systems. These include non-Newtonian fluids flow, rheological modelling of fibre and polymer systems, viscous fingering, and other chemically or thermally driven instabilities in porous media. He holds a Dilôme d'Ingénieur from the Ecole Centrale de Paris in France and M.Sc. and Ph.D. degrees from Stanford University.